JEM Journal of Experimental Medicine

BRIEF DEFINITIVE REPORT

B cell–intrinsic *Myd88* regulates disease progression in murine lupus

Jeremy S. Tilstra[1,2,3], Minjung Kim[1], Rachael A. Gordon[1,2], Claire Leibler[1], Haylee A. Cosgrove[1], Sheldon Bastacky[4], Kevin M. Nickerson[1], and Mark J. Shlomchik[1]

Nucleic acid–specific Toll-like receptors (TLRs) have been implicated in promoting disease pathogenesis in systemic lupus erythematosus (SLE). Whether such TLRs mediate disease onset, progression, or both remains undefined; yet the answer to this question has important therapeutic implications. MyD88 is an essential adaptor that acts downstream of IL-1 family receptors and most TLRs. Both global and B cell–specific *Myd88* deficiency ameliorated disease in lupus-prone mice when constitutively deleted. To address whether *Myd88* was needed to sustain ongoing disease, we induced B cell–specific deletion of *Myd88* after disease onset in MRL.Fas^{lpr} mice using an inducible Cre recombinase. B cell–specific deletion of *Myd88* starting after disease onset resulted in ameliorated glomerulonephritis and interstitial inflammation. Additionally, treated mice had reduced autoantibody formation and an altered B cell compartment with reduced ABC and plasmablast numbers. These experiments demonstrate the role of MyD88 in B cells to sustain disease in murine lupus. Therefore, targeting MyD88 or its upstream activators may be a viable therapeutic option in SLE.

Introduction

Systemic lupus erythematosus (SLE) is an autoimmune disease driven by immune dysregulation that results in end-organ damage. Nucleic acid–specific endosomal Toll-like receptors (TLRs)—namely TLR7, TLR8, and TLR9—have been implicated in SLE pathogenesis in numerous murine models and patients (Fillatreau et al., 2021; Jeong et al., 2018; Nickerson et al., 2010; Song et al., 2020; Wang et al., 2014; Zhang et al., 2021), and the X-linked regulation of TLR7/8 may contribute to sex bias in SLE pathogenesis (Fillatreau et al., 2021; Souyris et al., 2018; Umiker et al., 2014). Several components of the MyD88/TLR signaling pathway have been identified as risk alleles in SLE patients, including TLR7, TLR8, TLR9, IL-1 related kinase 1 (IRAK1), and interferon response factor 5 (IRF5) (Jeong et al., 2018; Song et al., 2020; Zhang et al., 2021). MyD88 is used by all TLRs (with the exception of TLR3) and IL-1–like receptors (Zhang et al., 2021). TLR signaling is mediated by MyD88, an adaptor protein that regulates disease pathogenesis in SLE (Teichmann et al., 2013). *Myd88*$^{-/-}$ MRL.Fas^{lpr} mice have markedly reduced autoimmunity with ameliorated nephritis and dermatitis, loss of autoantibody production, and dampened immune activation (Nickerson et al., 2010; Sadanaga et al., 2007). Furthermore, mice with deletion of both the TLR7 and TLR9 alleles recapitulated the majority of the Myd88$^{-/-}$ MRL.Fas^{lpr} phenotype, which suggests that MyD88 potentiation of disease resides downstream of these two endosomal TLRs (Nickerson et al., 2010) and is independent of IL-1 signaling (Loftus et al., 2023).

Subsequent work showed that B cell–specific *Myd88* signaling was responsible for promoting the majority of the lupus phenotype, with the notable exception of dermatitis, which was dependent on *Myd88* expressed in CD11c-positive cells (Teichmann et al., 2013). More recently, the negative regulatory role of TLR9 in SLE pathogenesis was also isolated to the B cell compartment, with no detectable effect among dendritic cells (DCs) (Tilstra et al., 2020).

Here, we set out to determine whether B cell–intrinsic *Myd88* is required for disease perpetuation even after disease initiation. We hypothesized that B cell–expressed *Myd88* is necessary for continued immune activation and tissue damage in SLE and possibly other diseases. This notion is supported by reports that B cell depletion, via anti-CD20 or CAR-T cells, results in improved disease in patients with SLE and in lupus mice (Furie et al., 2022; Kansal et al., 2019; Mackensen et al., 2022). An alternative hypothesis is that, once B cells and subsequently autoreactive T cells have been activated, they no longer require

[1]Department of Immunology, University of Pittsburgh School of Medicine, Pittsburgh, PA, USA; [2]Department of Medicine, University of Pittsburgh School of Medicine, Pittsburgh, PA, USA; [3]Lupus Center of Excellence, University of Pittsburgh School of Medicine, Pittsburgh, PA, USA; [4]Department of Pathology, University of Pittsburgh School of Medicine, Pittsburgh, PA, USA.

Correspondence to Mark J. Shlomchik: mshlomch@pitt.edu; Jeremy S. Tilstra: tilstraj@upmc.edu.

continued TLR stimulation to perpetuate the immune response. Supporting this hypothesis is the observation that autoreactive T cells recognizing nucleic acid–containing immune complexes can drive B cell proliferation even if they receive no TLR stimulation; however, the initiation of the cycle does require TLRs (Giles et al., 2015). Furthermore, many believe that SLE is mediated by long-lived plasma cells (PCs) and the autoantibody response (Alexander et al., 2015; Hiepe et al., 2011). Thus, once formed, these cells could potentiate disease without further stimulation. As long-lived PCs downregulate CD19 and CD20, these cells are not efficiently targeted by B cell promoter–driven Cre-lox systems or most B cell–depleting therapies (Ahuja et al., 2011). Thus, if this alternate hypothesis were true, targeting MyD88 in B cells in established autoimmune diseases would be ineffective.

To distinguish between these two hypotheses, we used a B cell–specific, tamoxifen-inducible Cre to delete *Myd88* after the onset of immune dysregulation and disease initiation in the MRL/lpr model of SLE. This methodology allowed us to determine the time-dependent contribution of B cell–intrinsic *Myd88* to ongoing disease and determine whether B cell–*Myd88* signaling is necessary for disease perpetuation and progression.

Results and discussion

Inducible B cell–specific *Myd88* deletion in MRL.Fas^{lpr} mice is efficient and blocks TLR signaling

To study the effect of time-dependent, B cell–specific deletion of *Myd88* in the MRL.Fas^{lpr} model, we crossed two alleles: the tamoxifen-inducible hCD20-Cre (Tam-hCD20-Cre), which allowed for inducible Cre activity specifically in B cells after tamoxifen administration (Khalil et al., 2012), and the *Myd88*-floxed allele (*Myd88^{fl}*). These mice will be referred to as Tam-hCD20-Cre;-*Myd88^{fl}* MRL.Fas^{lpr}. Controls in this study were Tam-hCD20-Cre negative *Myd88^{fl}* MRL.Fas^{lpr} mice, also treated with tamoxifen. Fig. 1 A schematizes the experimental design.

Quantitative PCR (qPCR) analysis of genomic *Myd88* in sorted cell populations from Tam-hCD20-Cre;-*Myd88^{fl}* MRL.Fas^{lpr} mice treated with tamoxifen for 3 wk (Fig. 1 B) resulted in 73.2% deletion of the *Myd88* allele in total B cells (CD19$^+$) without any significant deletion in T cells (CD90$^+$) or conventional DC (cDC) (CD11c$^+$). In contrast, among plasmablasts (PBs) (CD90$^-$, CD138$^+$, Kappa$^+$), there was a modest 17% reduction in *Myd88* alleles, which was not statistically significant. More importantly, at the functional level, B cells from the Tam-hCD20-Cre;-*Myd88^{fl}* MRL.Fas^{lpr} (treated with tamoxifen for 6–8 wk) failed to translocate NF-κB to the nucleus when stimulated by CpG-DNA (Fig. 1, C and D), indicating the functional impact of deletion of MyD88 in the B cells of these mice.

B cell–specific inducible *Myd88* deletion results in reduced autoantibody levels

Administering tamoxifen to female MRL.Fas^{lpr} and NZB/W mice is known to ameliorate disease (Sthoeger et al., 2003; Wu et al., 2000). To eliminate this confounding factor, we excluded female mice from the disease endpoint analysis.

Global *Myd88* deletion or deletion of *Myd88* in B cells alone results in the abrogation of both anti-RNA and anti-DNA antibodies (Nickerson et al., 2010; Teichmann et al., 2013). In our colony, MRL.Fas^{lpr} mice develop immune activation and renal inflammation by 11 wk of age (Tilstra et al., 2018). To confirm our earlier data, we compared the level of antibody production in MRL.Fas^{lpr} mice at 12 wk of age (just prior to intervention) to that of non-autoimmune C57Bl/6 mice (Fig. S1). As expected, 12-wk-old untreated MRL.Fas^{lpr} mice exhibit elevated titers of all assessed autoantibodies when compared to non-autoimmune Tam-hCD20-Cre B6 mice (Fig. S1).

To examine the role of B cell–specific deletion of *Myd88* on antibody production, we compared autoantibodies from Tam-hCD20-Cre;-*Myd88^{fl}* MRL.Fas^{lpr} with those of Cre negative controls after 8 wk of tamoxifen treatment, as well as to pretreatment levels (Fig. 2 A). While antibody titers significantly increased in control mice between 12 and 20 wk of age, there was no statistical increase in anti-DNA and anti-RNA autoantibody levels in tamoxifen-treated Tam-hCD20-Cre;-*Myd88^{fl}* MRL.Fas^{lpr} mice over the treatment course (Fig. 2 A), and only a slight increase in anti-Sm antibodies, with no high producers, in the treated group. The reduced autoantibody levels correlated with a reduction in antinuclear antibody (ANA) staining intensity in Tam-hCD20-Cre;-*Myd88^{fl}* MRL.Fas^{lpr} mice, with a homogenous pattern in all samples (Fig. 2 B).

The lack of increase in antibody formation suggests a static antibody-forming cell (AFC) function once *Myd88* is deleted. This is most likely because of preventing activation of autoreactive B cell precursors and hence preventing their differentiation into AFC. We recently showed that age-associated (ABC)-like B cells, which are TLR-dependent and are known to contain antinuclear specificities (Nickerson et al., 2023), are precursors of autoreactive PB in the MRL.Fas^{lpr} mouse; they express higher levels of TLR7 and can be activated by both TLR7 and TLR9 ligands (Leibler et al., 2022; Nickerson et al., 2023). As the Tam-hCD20-Cre does not directly target PBs (Ahuja et al., 2007; Fig. 1 B), residual autoantibodies could stem from continued secretion from PBs/PCs already formed at treatment onset. Alternatively, or in addition, these autoantibodies could be attributable to the high level of escape in the activated B cell population.

B cell–specific *Myd88* deletion after disease onset results in disease amelioration

The same cohorts of mice were assessed for several clinical markers of disease. There was no reduction in dermatitis in Tam-hCD20-Cre;-*Myd88^{fl}* MRL.Fas^{lpr} mice treated with tamoxifen (Fig. 3 A), consistent with our prior study examining constitutive B cell–specific deletion of Myd88 (Teichmann et al., 2013). However, there was a significant reduction in kidney disease in treated mice. There was a significant decrease in proteinuria and a more robust and significant reduction in both glomerulonephritis and interstitial disease as assessed by histologic evaluation (Fig. 3, B–E), as was determined by mesangial cell proliferation, crescent formation, hypercellularity, glomerular enlargement, and interstitial inflammation. We further observed a reduction in spleen and a trend toward reduced lymph node weights (Fig. 3, F and G), which has been associated

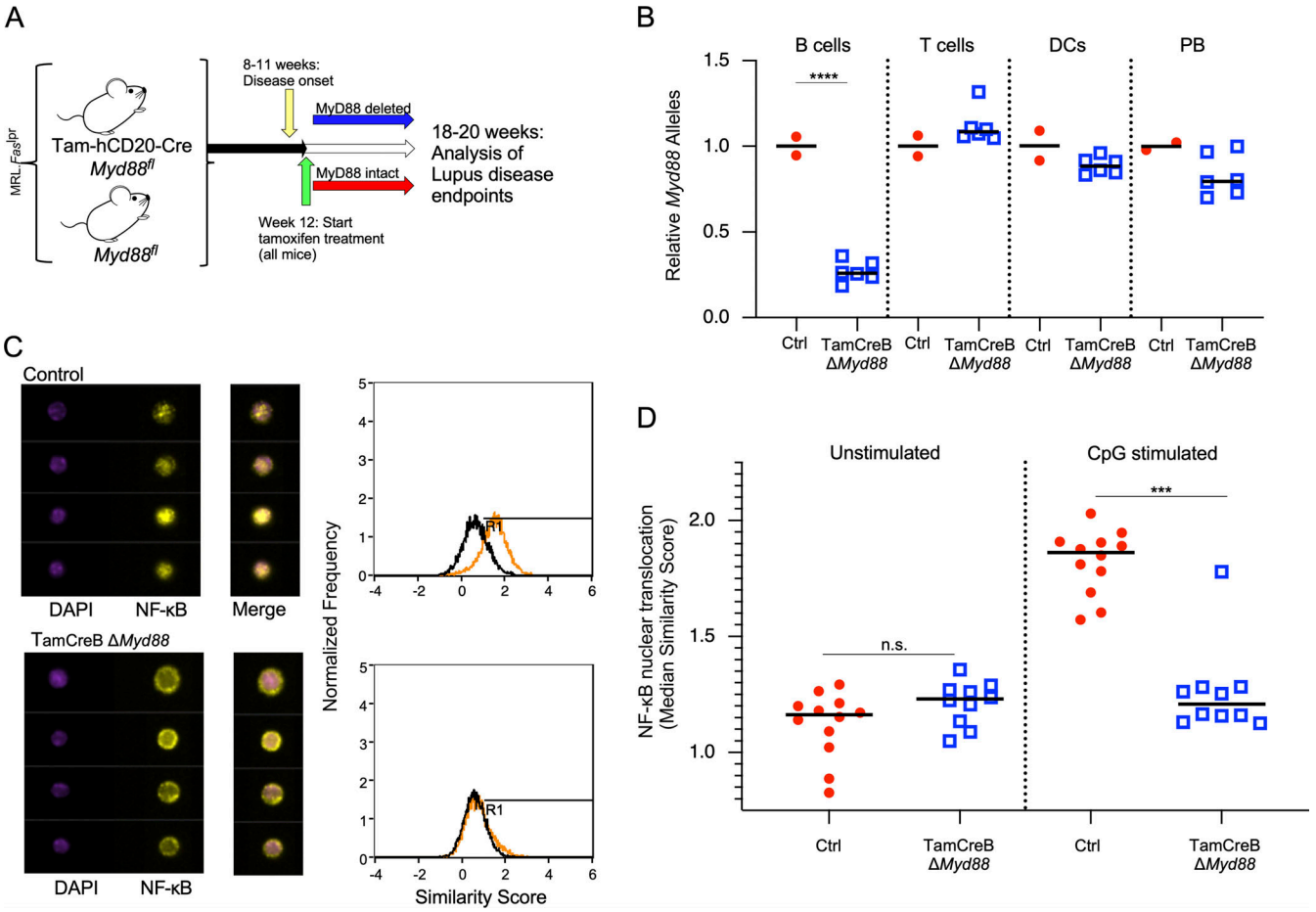

Figure 1. **Tamoxifen-induced deletion of *Myd88* in B cells results in suppressed MyD88 activity. (A)** Schematic of experimental design; Tam-hCD20-Cre;-*Myd88*^{fl} MRL.Fas^{lpr} or Cre negative controls were aged up to 12 wk of age, an early disease time point. Mice were then treated 2× per week with tamoxifen 1 mg in corn oil for 8 wk, after which mice were euthanized and assessed for disease endpoints. **(B)** Tam-hCD20-Cre;-*Myd88*^{fl} MRL.Fas^{lpr} (TamCreB Δ*Myd88*) (n = 6) or Cre negative controls (Ctrl) (n = 2) were treated for 3 wk with tamoxifen given by oral gavage. Splenocytes were then sorted and analyzed for *Myd88* allelic presence by qPCR in the cell populations as indicated: B cells (CD19$^+$, CD90$^-$ cells), T cells (CD90$^+$, CD19$^-$), cDC (CD19$^-$, CD11c$^+$), and PBs (CD90$^-$, CD138$^+$, Kappa^{high}). **(C)** Splenocytes were isolated from Tam-hCD20-Cre;-*Myd88*^{fl} MRL.Fas^{lpr} (n = 10) or Cre-negative controls (n = 12) and stimulated with CpG DNA (10 µg/ml) for 2 h. Nuclear translocation of NF-κB, a downstream signaling component of the MyD88 pathway, was assessed by Amnis imaging cytometer. In the left panel, representative images of NF-κB and nuclear stain (DAPI) in CD19$^+$ B cells are shown along with representative histograms on the right outlining the NF-κB location relative to the nuclear stain, with colocalization of DAPI and NF-κB signifying activation (represented by a shift of the orange/stimulated histogram to a higher similarity score, representing the overlap between NF-κB and DAPI) with the maintenance of NF-κB in the cytoplasm representing lack of activation (represented by overlap of black (unstimulated) and orange (stimulated) similarity scores on the associated histogram). **(D)** The median similarity score represents NF-κB nuclear translocation and was graphed for a subset of treated and control mice. Scatter plots display data from individual mice with black lines showing median values. ***P < 0.001, ****P < 0.0001, two-tailed Mann–Whitney *U* test. Data shown are representative of two independent experiments with n indicated for each experiment shown.

with improved outcomes in the MRL.Fas^{lpr} mice (Shlomchik et al., 1994). Overall, this suggests that disease progression requires continued TLR/MyD88 signaling in the B cell compartment.

To examine a potential concern that activation of the Tam-hCD20-Cre may have impacts on the B cell compartment, we generated a cohort of Tam-hCD20-Cre MRL.Fas^{lpr} and Cre-negative MRL.Fas^{lpr} mice (both without an associated floxed *Myd88* allele). These mice were also treated with tamoxifen starting at 12 wk of age for 8 wk. Notably, tamoxifen treatment of Tam-hCD20-Cre MRL.Fas^{lpr} mice resulted in no significant alterations in autoantibody production (Fig. S2, A–C). Furthermore, these mice neither exhibited any significant improvement in clinical markers of dermatitis or renal disease (Fig. S2, D–G) nor spleen weight (Fig. S2 H). Only a slight decrease in lymph node weight was observed in this cohort (Fig. S2 I). These data suggest that activation of Tam-hCD20-Cre alone had no significant impact on disease phenotype or B cell function.

B cell–specific *Myd88* deletion after disease onset results in altered AFC populations

There was a nearly twofold reduction in AFCs, with a fourfold reduction in PBs as a percentage of the B cell compartment (TCR$^-$, CD138$^+$, CD44^{high}, P < 0.005) and a 1.8-fold reduction in the percentage of ABC-like B cells in the B cell compartment (CD19$^+$CD11b$^+$CD11c$^+$, P < 0.001) between treated Tam-hCD20-

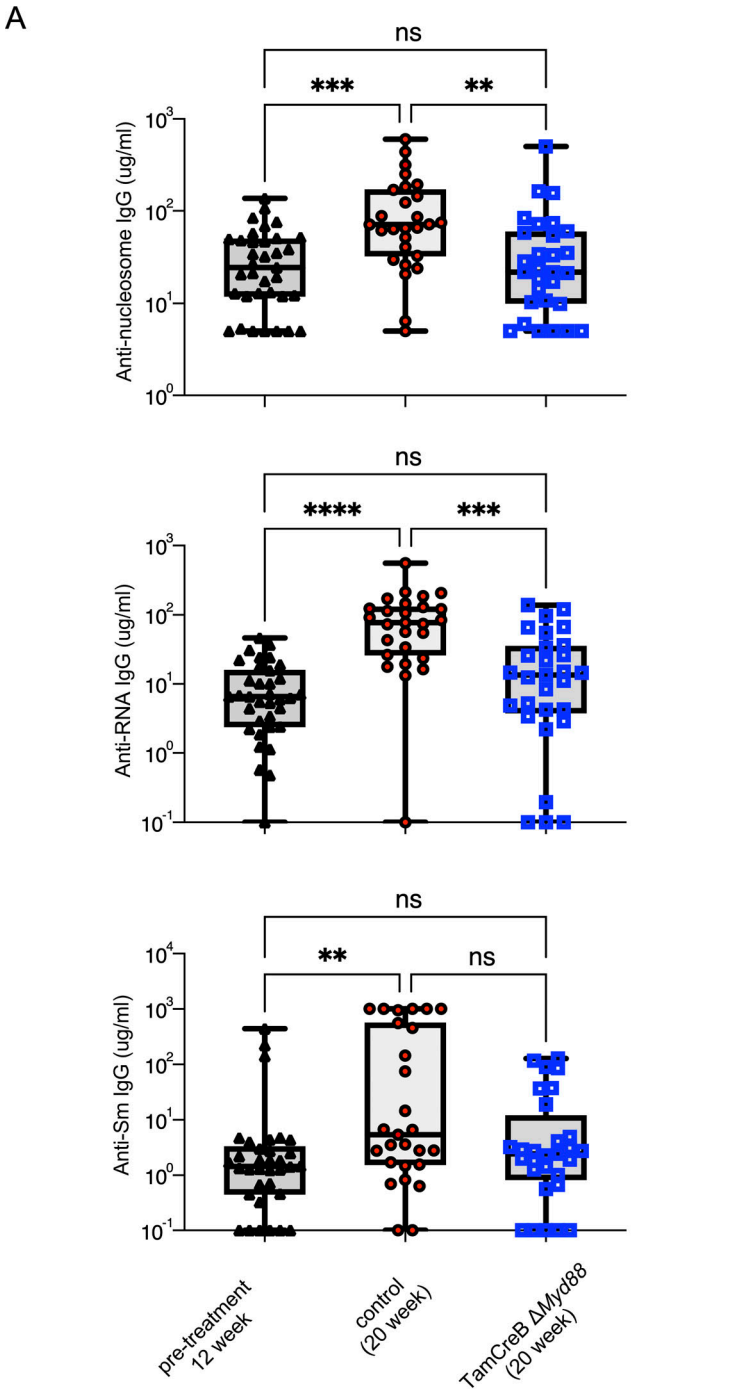

Figure 2. **B cell–intrinsic deletion of *Myd88* suppresses autoantibody formation after disease onset and formation of ANA$^+$ B cells. (A)** Serum concentrations of anti-nucleosome, anti-RNA, and anti-Sm in MRL.Fas^{lpr} mice at 12 wk of age prior to experimental intervention (n = 34–35), Tam-hCD20-Cre;-Myd88fl MRL.*Fas*^{lpr} (TamCreB ΔMyd88) (n = 29), and Cre negative controls after 8 wk of tamoxifen treatment (n = 27) aimed at suppressing *Myd88* in the B cell compartment. Scatter plots display data from individual mice with black lines showing median values. **P < 0.01, ***P < 0.001, ****P < 0.0001, Kruskal–Wallis with multiple corrections. **(B)** Representative HEp-2 ANA staining from the serum of male; Tam-hCD20-Cre;-*Myd88*^{fl} MRL.Fas^{lpr} or Cre negative controls at 20 wk of age after 8 wk of tamoxifen treatment (images are 100× with scale bar representing 50 µm). Data shown are representative of three independent cohorts with data combined from all cohorts and n indicated for each experiment as shown.

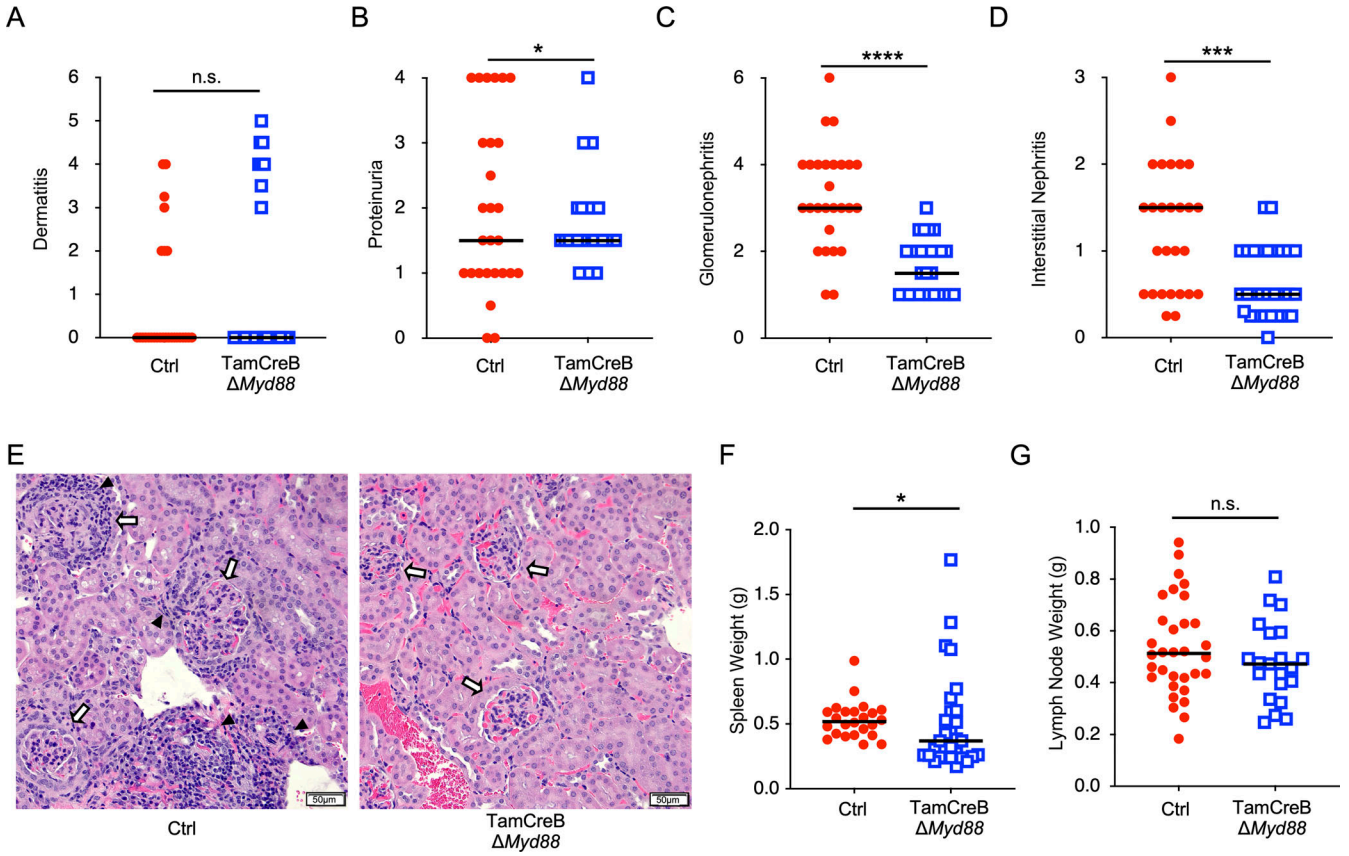

Figure 3. **B cell–specific *Myd88* deletion after disease onset results in ameliorated kidney disease. (A–E)** Phenotypic markers of disease were assessed in 20-wk-old male Tam-hCD20-Cre;-*Myd88*^{fl} MRL.Fas^{lpr} (TamCreB Δ*Myd88*) (n = 29) or Cre negative (Ctrl) (n = 27) MRL.Fas^{lpr} mice after 8 wk of tamoxifen treatment including (A) dermatitis, (B) proteinuria, (C) glomerular renal disease, (D) interstitial and perivascular renal infiltrates, with (E) representative images of H&E kidney sections from mice of indicated genotype, with black arrowheads indicating interstitial infiltrates and white arrows indicated glomeruli (images are 200× with scale bars representing 50 μm). **(F and G)** Additional phenotypic endpoints were assessed for each noted genotype including (F) spleen weight and (G) lymph node weight. Scatter plots display data from individual mice with horizontal lines showing median values. *P < 0.05, ***P < 0.001, ****P < 0.0001, two-tailed Mann–Whitney *U* test, except for proteinuria and dermatitis which were assessed by Chi-squared analysis given their bimodal distribution. Data shown are representative of three independent cohorts with data combined from all cohorts and *n* indicated for each experiment as shown.

Cre;-*Myd88*^{fl} MRL.Fas^{lpr} mice and controls (Fig. 4, A and B). In the cohort of tamoxifen-treated Tam-hCD20-Cre;-*Myd88*^{fl} MRL.Fas^{lpr}, we observed a reduction in the total number of cells of all lineages in the spleen as assessed by spleen weight. There was no difference in the percentage of B cells amongst total splenocytes (Fig. 4 C) nor was there an altered distribution of marginal zone or follicular B cells between Tam-hCD20-Cre;-*Myd88*^{fl} MRL.Fas^{lpr} mice and controls. Given the unexpected decrease in ABCs and PBs, it was important to determine the deletion efficiency of these more terminally differentiated subsets. After 8 wk of treatment with tamoxifen, 67% of CD19^{+} B cells maintained allelic deletion of *Myd88*. However, in the ABC compartment, *Myd88* deletion efficiency was reduced to just over 50% and was reduced to only 26% in the PB compartment (Fig. 4 E). Those mice that exhibited more escape in the total B cell compartment tended to have higher levels of escape in the ABC and PB compartment. Among those mice with >70% deletion of Myd88 in the B cell compartment, only one of these had >32% escape in the ABC compartment (Fig. 4 F); whereas all but one mouse had >50% allelic expression among PB.

Despite significant alterations in these B cell populations, there were no specific changes in the splenic T cell populations, no alterations in the percent of CD4, CD8, or DN T cell populations, nor alterations in the naive, activated, and memory states of CD4 and CD8 T cell subsets (Fig. S3, A–C). Additionally, we did not observe any significant alteration in the percent of myeloid populations, including cDCs, plasmacytoid DCs (pDCs), or CD11b^{+} subsets, in the Tam-hCD20-Cre;-*Myd88*^{fl} MRL.Fas^{lpr} mice when compared with control animals (Fig. S3, D–G)

In this work, we use an engineered inducible genetic deletion system to demonstrate the continued role of B cell–specific *Myd88* in perpetuating disease. Targeting B cell–intrinsic *Myd88* after disease onset resulted in the amelioration of numerous disease features, including lymphoproliferation, antibody formation, and most importantly, renal disease as defined by reduced glomerulonephritis and interstitial infiltration. These findings give us a greater understanding of SLE progression and confirm a role for continual TLR signaling in murine lupus (and likely other autoimmune diseases). Critically, these results can also provide a future therapeutic design for the treatment of SLE patients.

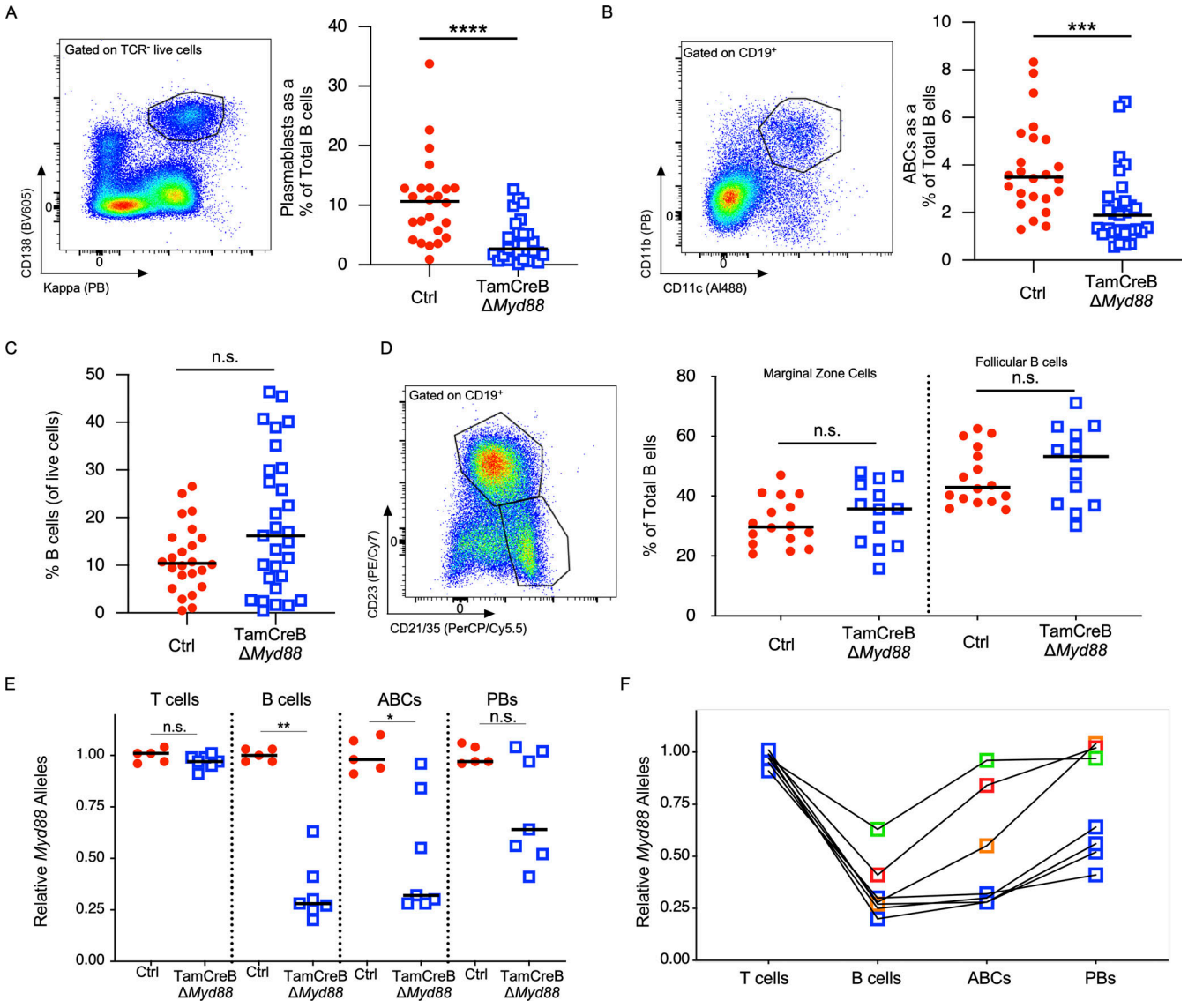

Figure 4. **AFCs and ABCs are reduced in mice with B cell–specific *Myd88* deletion.** The B cell compartment was analyzed for 20-wk-old male Tam-hCD20-Cre;-*Myd88*^{fl} MRL.Fas^{lpr} (TamCreB Δ*Myd88*) (*n* = 29) or Cre negative (Ctrl) (*n* = 27) MRL.Fas^{lpr} mice after 8 wk of tamoxifen treatment. **(A)** Left panel shows the gating strategy for PBs (TCR^{-}CD138^{+},Kappa^{high}) B cells with % of each subset represented on the right panel. **(B)** Left panel shows the gating strategy for age-associated B cells (CD19^{+}CD11c^{+} CD11b^{+}) with % of each subset represented on the right panel. **(C)** B cells as a percent of total splenocytes were measured and gated as CD19^{+} cells. **(D)** Left panel shows gating strategy for follicular (CD19^{+}, CD23^{+}, CD21/35^{int}) and marginal zone (CD19^{+}CD23^{-},CD21/35^{high}) B cells with % of each subset represented on the right panel. **(E and F)** Tam-hCD20-Cre;-*Myd88*^{fl} MRL.Fas^{lpr} (TamCreB Δ*Myd88*) (*n* = 7) or Cre negative controls (Ctrl) (*n* = 5) were treated for 8 wk with tamoxifen given by oral gavage. Splenocytes were then sorted and analyzed for *Myd88* allelic presence by qPCR in the cell populations as indicated: T cells (CD90^{+}, CD19^{-}), B cells (CD19^{+}, CD90^{-},CD11c^{-},CD11b^{-},CD138^{-} cells), ABCs (CD19^{+},CD11c^{+},CD11b^{+},CD138^{-}), and PB (CD90^{-}, CD138^{+}, CD44^{+}). In E, deletion efficiency was compared between experimental or control mice, and in F, deletion efficiency in each subset was compared amongst individual TamCreB Δ*Myd88* mice. Scatter plots display data from individual mice with horizontal lines showing median values. *P < 0.05, **P < 0.01, ***P < 0.001, ****P < 0.0001, two-tailed Mann–Whitney *U* test. Data shown are representative of three independent cohorts with data combined from all cohorts and *n* indicated for each experiment as shown.

Others and we have previously shown that immune cells are activated prior to 11 wk of age in MRL.Fas^{lpr} mice (Liu et al., 2006; Sakić et al., 1992; Tilstra et al., 2018). In this study, at the time of intervention, B cells had begun to make substantial levels of autoantibodies. Giles et al. had previously shown that pre-activated antinuclear reactive T cells can drive the proliferation of B cells that present their cognate antigen, independent of TLR signaling (Giles et al., 2017). Based on this work, we felt that it was a possibility that these IC-dependent autoreactive T cells could override the need for TLR signals and continue to drive the B cell response in the absence of TLR/MyD88 signaling, once initial TLR-dependent activation had occurred. While murine studies have shown a clear dependence of lupus pathogenesis on T cells (Gilkeson et al., 1992; Peng et al., 1998; Wofsy, 1986), our study suggests that continued B cell activation through MyD88 signaling pathways is also required for disease perpetuation.

The ABC population, which depends on TLR signals to develop (Jenks et al., 2018; Nickerson et al., 2023), was substantially

reduced in treated mice. Several groups have implicated ABCs in the development of SLE (Jenks et al., 2018; Liu et al., 2017; Ricker et al., 2021; Rubtsova et al., 2017) as well as their dependency on TLR signaling (Jenks et al., 2019; Ricker et al., 2021). Our group has recently shown that ABCs in MRL.*Fas*^{lpr} mice are rapidly turning over, even though they in some respects have the phenotype of a memory B cell. Further, we showed that specific deletion of ABC can reduce disease phenotypes (Nickerson et al., 2023). Whether reductions in ABC numbers upon treatment of diseased Tam-hCD20-Cre;-*Myd88*^{fl} MRL.Fas^{lpr} mice are due to deletion, reduced proliferation, or inhibited function cannot be determined in this model system. Regardless of the reasons for cellular loss, these findings support the idea that the majority of ABC development requires continued TLR signaling, consistent with the dynamic nature of the population (Nickerson et al., 2023). Indeed, we find progressive deletion escape at each stage of B cell differentiation, increasing from 33% (B cells) to 50% (ABCs) to 75% (PBs). However, as four of the seven assessed mice exhibited allelic deletion >50% in the ABC compartment (Fig. 4 F), this would at a minimum suggest that at least a portion of ABCs develop and/or are maintained in the absence of MyD88 signaling. Further, PBs exhibit significantly lower degrees of *Myd88* deletion after tamoxifen administration, with almost all mice having at least 50% allelic escape, suggesting that PB formation/differentiation requires at least one intact *Myd88* allele. If *Myd88* were not important, then the frequency of undeleted alleles would have mirrored that in the naïve B cell precursor population.

The selective expansion of B cells and PBs with undeleted *Myd88* also likely explains why autoantibody levels merely stabilize after tamoxifen treatment but do not fall to non-autoimmune levels. Commensurately, ABC could be an important APC for autoreactive T cells (Rubtsov et al., 2011; Rubtsova et al., 2017); however, incomplete deletion of *Myd88* in these cells may explain the lack of significant alterations in the T cell compartment in this study. Alternatively, or in addition, once activated at least 12 wk prior to effective treatment, autoreactive and activated memory T cells may remain or even further expand without the need for additional stimulation by B cell APCs. One qualification regarding the T cell compartment evaluation is that in murine models of SLE as well as human patients, the target antigens of autoreactive T cells are undefined; therefore, we are unable to assess antigen-specific T cell responses and thus may miss subtle differences within this T cell compartment. In addition to their role as APCs and activators of autoreactive T cells, B cells, in general, and ABCs, specifically, are known to secrete inflammatory cytokines such as TNF, IFNγ, and IL-17 (Mouat et al., 2022). Thus, a reduction in these cytokines may define another mechanism by which B cell–specific *Myd88* may modulate disease in this system.

Based on the significant amelioration of disease in this model, we suggest that the TLR/MyD88 pathway may be a therapeutic target for reducing nephritis in SLE patients. In fact, hydroxychloroquine, a mainstay treatment for SLE patients, is known to suppress TLR7 and TLR9 signaling upstream of MyD88 through intercalation into nucleotides (Kuznik et al., 2011). Given this potential mode of action, our findings would suggest that hydroxychloroquine would need to act specifically in the B cell compartment.

The data herein also add to recent data suggesting that B cell–targeting therapy is efficacious in the treatment of SLE. This is despite early failures when examining phase III trials focusing on rituximab (B cell–depleting therapy; Rovin et al., 2012). The failure of rituximab was likely complicated by incomplete B cell depletion rather than B cells being an inappropriate target (Ahuja et al., 2011). However, more recent studies support the important role of B cells in the treatment of SLE. This includes human studies in which belimumab, which targets the B cell survival factor BAFF, resulting in improved kidney outcomes in lupus patients (Furie et al., 2020; Rovin et al., 2022). Similarly, a phase II study in which anti-CD20 therapy mediated B cell depletion using Obinutuzumab was effective for treating lupus nephritis (Furie et al., 2022). Finally, recent exciting data in five patients with treatment-resistant lupus nephritis showed that CAR-T cell therapy targeting CD19^{+} cells resulted in a rapid improvement in disease. Although encouraging, there are still significant possible side effects of pan–B cell depletion. Patients with defective *Myd88* expression are at high risk for pyogenic infections (von Bernuth et al., 2008); however, this current work suggests that even incomplete MyD88 suppression specifically in B cells is sufficient to reduce disease, likely rebalancing the overactive immune response. Furthermore, this work supports the future efficacy of the TLR7/8 or TLR7/8/9 antagonist. We and others have shown that these TLRs are specifically implicated in SLE pathogenesis and are the major mediators of MyD88 activation in murine and likely human SLE (Fillatreau et al., 2021). Therefore, approaches targeting the MyD88 signaling pathway in B cells have the potential to be both more specific and a safer approach to suppressing autoreactive B cells in lupus nephritis compared to complete deletion, a concept now supported by our model in which intervention after disease onset showed a benefit.

Materials and methods

Flow cytometry

Flow cytometry was performed as previously described (Tilstra et al., 2020), with the exception that cells were resuspended in 0.5% bovine serum albumin, phosphate-buffered saline (PBS), 25 mM HEPES, and 2.5 mM EDTA.

Measurement of serum antibodies

HEp-2 immunofluorescence assays (Antibodies Inc. or Bio-Rad) were performed as previously described (Christensen et al., 2006) with the serum diluted at 1:200. Images were captured on an Olympus IX83. Image display settings and exposure times were kept constant for all samples using CellSens software (Olympus). Anti-nucleosome, anti-Sm, and anti-RNA concentrations were measured by ELISA as previously described (Gordon et al., 2017).

qRT-PCR

For assessing the deletion efficiency of *Myd88*, qRT-PCR was performed on genomic DNA extracted from FACS-sorted cells.

The amount of DNA encoding *Myd88* in each sample was normalized to that of the unaffected gene *Actb*. Primer sequences are *Myd88* forward 5′-CGGAACTTTTCGATGCCTTT-3′ and reverse 5′-CACACACAACTTAAGCCGAT-3′, β-actin forward 5′-GGCTGTATTCCCCTCCATCG-3′, reverse 5′-CCAGTTGGTAAC AATGCCATGT-3′. qRT-PCR was performed with Agilent Brilliant II SYBR Green qPCR kit on Roche LightCycler 96.

Ex vivo stimulation

Splenocytes from indicated mice as noted in individual figures were isolated as per flow cytometry methods. Cells were rested in complete RPMI (RPMI + 10% Fetalplex, penicillin/streptomycin, Glutamax, HEPES, and 50 µM 2-mercaptoethanol) for 45 min then stimulated with the 10 µg/ml CpG DNA (CpG ODN 1826; Hokkaido System Science) for 2 h. Cells were then fixed with 1.5% paraformaldehyde followed by permeabilization with PBS with 5% BSA, HEPES, EDTA, and 0.1% Triton-X. Cells were stained with unconjugated rabbit anti-NFκB p-65 (D14E12; Cell Signaling), followed by anti-rabbit IgG-Cy3 (polyclonal; Invitrogen), CD45R-APC-Cy7 (RA3-6B2; BD Pharmingen), TCRβ-APC (H57-597; Tonbo), and DAPI. Samples were run on an ImagestreamX MkII Imaging Flow Cytometer (Amnis) and analyzed using the nuclear translocation wizard in the IDEAS software (Amnis).

Evaluation of clinical disease

An assessment was performed as described in Tilstra et al. (2020). Briefly, proteinuria was measured by Albustix strips. Glomerular and interstitial nephritis were scored by a pathologist (S. Bastacky) in a blinded manner. Dermatitis was scored based on the extent of dermatitis on the dorsum of the neck and back. Macroscopic surface area was scored from 0 to 5 for an affected area up to 9.1 cm^2, with up to one additional point for the presence of ear (1/4 point each) and muzzle (1/2 point) dermatitis.

Reagents

Antibodies used for FACS surface and intracellular staining are given in Table 1.

Mice

hCD20-Tamoxifen inducible Cre (Tam-hCD20-Cre) MRL.Fas^{lpr} mice were generated previously (Wen et al., 2016) and either used as a control or intercrossed with Myd88fl MRL.Fas^{lpr} mice (Teichmann et al., 2013). Both strains had been backcrossed onto the MRL.Fas^{lpr} lupus susceptible strain >10 generations. Tam-hCD20-Cre C57Bl/6 mice were used as additional controls as indicated. Mice in the experimental cohorts were treated with 1 mg of tamoxifen daily by oral gavage 2× per week. Tamoxifen (cat no. 156738; MP Biomedicals) was diluted at a concentration of 10 mg/ml in corn oil (C8267; Sigma-Aldrich) after 2 h at 37°.

Statistical analysis

Statistics were calculated in GraphPad Prism by one-tailed or two-tailed Mann–Whitney *U* test or ANOVA with Kruskal–Wallis for multiple comparisons was used as indicated throughout. For variables with bimodal distribution (proteinuria and dermatitis) Chi-squared analysis was used. P values are represented as *P < 0.05, **P < 0.01, ***P < 0.001, ****P < 0.0001.

Table 1. **Antibodies used for FACS surface and intracellular staining**

Name	Fluorophore	Clone	Company
CD11b	PE	M1/70	BioLegend
CD11b	Biotin	M1/70	Conjugated in house
CD11c	Al488	N418	Conjugated in house
CD11c	PE/Cy7	N418	BioLegend
CD138	BV605	281-2	BD Horizon
CD138	PE	281-2	BioLegend
CD19	APC-Cy7	1D3	BD Pharmingen
CD19	BUV395	1D3	BD Horizon
CD19	Al647	1D3	BD Pharmingen
CD21/CD35	PerCP/Cy5.5	7E9	Conjugated in house
CD23	PE/Cy7	B3B4	BioLegend
CD317	PE	927	BioLegend
CD38	PE	90	BioLegend
CD4	PE	GK1.5	BioLegend
CD44	Al488	Pgp-1	Conjugated in house
CD44	BV605	Pgp-1	BD Horizon
CD62L	PE/Cy7	MEL-14	BioLegend
CD8	Al647	TIB105	Conjugated in house
CD90.2	Al488	30H12	Conjugated in house
F4/80	F4/80	Al647	Conjugated in house
Kappa	Pacific Blue	187.1	Conjugated in house
Kappa	Pacific Blue	187.1	Conjugated in house
Ly-6G/Ly-6C	PE/Cy7	RB6-8C5	BioLegend
SA	APC-eFluor780		eBioscience
Siglec H	Al647	551	BioLegend
TCRβ	APC/Cy7	H57-597	BioLegend

Study approval

All work was approved by the University of Pittsburgh Institutional Animal Care and Use Committee.

Online supplemental material

Fig. S1 shows autoantibodies that are present in 12-wk MRL.Fas^{lpr} compared with non-autoimmune mice. Fig. S2 shows that the activation of Tam-hCD20-Cre alone produced no significant impact on disease phenotype in murine SLE. Fig. S3 shows that myeloid and T cell distribution and activation profile are not significantly different in mice with B cell–specific *Myd88* deletion.

Data availability

All data from this manuscript will be made freely available upon request.

Acknowledgments

We would like to acknowledge the significant contributions of the technical work by Xiaoyan Gong to help complete this work. We would also like to recognize the assistance of the Flow Cytometry Core and the excellent animal care provided by the Department of Laboratory Animal Research.

This research was supported by National Institutes of Health grant R37AI118841 (to M.J. Shlomchik). J.S. Tilstra was funded by the National Institutes of Health Career Development Awards 5KL2TR001856-02 and 1K08AR075056-01.

Author contributions: J.S. Tilstra, R.A. Gordon, K.M. Nickerson, and M.J. Shlomchik conceived the project and designed experiments. M. Kim was responsible for mouse breeding and treating mice, as well as performing ELISA. J.S. Tilstra analyzed the flow data. J.S. Tilstra and M. Kim analyzed the qPCR data. C. Leibler and H.A. Cosgrove optimized AMNIS NF-κB activity data. S. Bastacky conducted a pathologic analysis of the kidney tissue. J.S. Tilstra and M.J. Shlomchik wrote the manuscript.

Disclosures: The authors declare no competing interests exist.

Submitted: 14 February 2023
Revised: 26 July 2023
Accepted: 11 September 2023

References

Ahuja, A., J. Shupe, R. Dunn, M. Kashgarian, M.R. Kehry, and M.J. Shlomchik. 2007. Depletion of B cells in murine lupus: Efficacy and resistance. *J. Immunol.* 179:3351–3361. https://doi.org/10.4049/jimmunol.179.5.3351

Ahuja, A., L.L. Teichmann, H. Wang, R. Dunn, M.R. Kehry, and M.J. Shlomchik. 2011. An acquired defect in IgG-dependent phagocytosis explains the impairment in antibody-mediated cellular depletion in Lupus. *J. Immunol.* 187:3888–3894. https://doi.org/10.4049/jimmunol.1101629

Alexander, T., R. Sarfert, J. Klotsche, A.A. Kühl, A. Rubbert-Roth, H.M. Lorenz, J. Rech, B.F. Hoyer, Q. Cheng, A. Waka, et al. 2015. The proteasome inhibitior bortezomib depletes plasma cells and ameliorates clinical manifestations of refractory systemic lupus erythematosus. *Ann. Rheum. Dis.* 74:1474–1478. https://doi.org/10.1136/annrheumdis-2014-206016

Christensen, S.R., J. Shupe, K. Nickerson, M. Kashgarian, R.A. Flavell, and M.J. Shlomchik. 2006. Toll-like receptor 7 and TLR9 dictate autoantibody specificity and have opposing inflammatory and regulatory roles in a murine model of lupus. *Immunity*. 25:417–428. https://doi.org/10.1016/j.immuni.2006.07.013

Fillatreau, S., B. Manfroi, and T. Dörner. 2021. Toll-like receptor signalling in B cells during systemic lupus erythematosus. *Nat. Rev. Rheumatol.* 17:98–108. https://doi.org/10.1038/s41584-020-00544-4

Furie, R., B.H. Rovin, F. Houssiau, A. Malvar, Y.K.O. Teng, G. Contreras, Z. Amoura, X. Yu, C.C. Mok, M.B. Santiago, et al. 2020. Two-year, randomized, controlled trial of belimumab in lupus nephritis. *N. Engl. J. Med.* 383:1117–1128. https://doi.org/10.1056/NEJMoa2001180

Furie, R.A., G. Aroca, M.D. Cascino, J.P. Garg, B.H. Rovin, A. Alvarez, H. Fragoso-Loyo, E. Zuta-Santillan, T. Schindler, P. Brunetta, et al. 2022. B-Cell depletion with obinutuzumab for the treatment of proliferative lupus nephritis: A randomised, double-blind, placebo-controlled trial. *Ann. Rheum. Dis.* 81:100–107. https://doi.org/10.1136/annrheumdis-2021-220920

Giles, J.R., M. Kashgarian, P.A. Koni, and M.J. Shlomchik. 2015. B cell-specific MHC class II deletion reveals multiple nonredundant roles for B cell antigen presentation in murine lupus. *J. Immunol.* 195:2571–2579. https://doi.org/10.4049/jimmunol.1500792

Giles, J.R., A.T. Neves, A. Marshak-Rothstein, and M.J. Shlomchik. 2017. Autoreactive helper T cells alleviate the need for intrinsic TLR signaling in autoreactive B cell activation. *JCI Insight*. 2:e90870. https://doi.org/10.1172/jci.insight.90870

Gilkeson, G.S., R. Spurney, T.M. Coffman, R. Kurlander, P. Ruiz, and D.S. Pisetsky. 1992. Effect of anti-CD4 antibody treatment on inflammatory arthritis in MRL-lpr/lpr mice. *Clin. Immunol. Immunopathol.* 64:166–172. https://doi.org/10.1016/0090-1229(92)90195-T

Gordon, R.A., J.M. Herter, F. Rosetti, A.M. Campbell, H. Nishi, M. Kashgarian, S.I. Bastacky, A. Marinov, K.M. Nickerson, T.N. Mayadas, and M.J. Shlomchik. 2017. Lupus and proliferative nephritis are PAD4 independent in murine models. *JCI Insight*. 2:e92926. https://doi.org/10.1172/jci.insight.92926

Hiepe, F., T. Dorner, A.E. Hauser, B.F. Hoyer, H. Mei, and A. Radbruch. 2011. Long-lived autoreactive plasma cells drive persistent autoimmune inflammation. *Nat. Rev. Rheumatol.* 7:170–178. https://doi.org/10.1038/nrrheum.2011.1

Jenks, S.A., K.S. Cashman, M.C. Woodruff, F.E. Lee, and I. Sanz. 2019. Extrafollicular responses in humans and SLE. *Immunol. Rev.* 288:136–148. https://doi.org/10.1111/imr.12741

Jenks, S.A., K.S. Cashman, E. Zumaquero, U.M. Marigorta, A.V. Patel, X. Wang, D. Tomar, M.C. Woodruff, Z. Simon, R. Bugrovsky, et al. 2018. Distinct effector B cells induced by unregulated toll-like receptor 7 contribute to pathogenic responses in systemic lupus erythematosus. *Immunity*. 49:725–739.e6. https://doi.org/10.1016/j.immuni.2018.08.015

Jeong, D.Y., S.W. Lee, Y.H. Park, J.H. Choi, Y.W. Kwon, G. Moon, M. Eisenhut, A. Kronbichler, and J.I. Shin. 2018. Genetic variation and systemic lupus erythematosus: A field synopsis and systematic meta-analysis. *Autoimmun. Rev.* 17:553–566. https://doi.org/10.1016/j.autrev.2017.12.011

Kansal, R., N. Richardson, I. Neeli, S. Khawaja, D. Chamberlain, M. Ghani, Q.U. Ghani, L. Balazs, S. Beranova-Giorgianni, F. Giorgianni, et al. 2019. Sustained B cell depletion by CD19-targeted CAR T cells is a highly effective treatment for murine lupus. *Sci. Transl Med.* 11:eaav1648. https://doi.org/10.1126/scitranslmed.aav1648

Khalil, A.M., J.C. Cambier, and M.J. Shlomchik. 2012. B cell receptor signal transduction in the GC is short-circuited by high phosphatase activity. *Science*. 336:1178–1181. https://doi.org/10.1126/science.1213368

Kuznik, A., M. Bencina, U. Svajger, M. Jeras, B. Rozman, and R. Jerala. 2011. Mechanism of endosomal TLR inhibition by antimalarial drugs and imidazoquinolines. *J. Immunol.* 186:4794–4804. https://doi.org/10.4049/jimmunol.1000702

Leibler, C., S. John, R.A. Elsner, K.B. Thomas, S. Smita, S. Joachim, R.C. Levack, D.J. Callahan, R.A. Gordon, S. Bastacky, et al. 2022. Genetic dissection of TLR9 reveals complex regulatory and cryptic proinflammatory roles in mouse lupus. *Nat. Immunol.* 23:1457–1469. https://doi.org/10.1038/s41590-022-01310-2

Liu, J., G. Karypis, K.L. Hippen, A.L. Vegoe, P. Ruiz, G.S. Gilkeson, and T.W. Behrens. 2006. Genomic view of systemic autoimmunity in MRLlpr mice. *Genes Immun.* 7:156–168. https://doi.org/10.1038/sj.gene.6364286

Liu, Y., S. Zhou, J. Qian, Y. Wang, X. Yu, D. Dai, M. Dai, L. Wu, Z. Liao, Z. Xue, et al. 2017. T-bet^{+}CD11c^{+} B cells are critical for antichromatin immunoglobulin G production in the development of lupus. *Arthritis Res. Ther.* 19:225. https://doi.org/10.1186/s13075-017-1438-2

Loftus, S.N., J. Liu, C.C. Berthier, J.E. Gudjonsson, M. Gharaee-Kermani, L.C. Tsoi, and J.M. Kahlenberg. 2023. Loss of interleukin-1 beta is not protective in the lupus-prone NZM2328 mouse model. *Front. Immunol.* 14:1162799. https://doi.org/10.3389/fimmu.2023.1162799

Mackensen, A., F. Müller, D. Mougiakakos, S. Böltz, A. Wilhelm, M. Aigner, S. Völkl, D. Simon, A. Kleyer, L. Munoz, et al. 2022. Anti-CD19 CAR T cell therapy for refractory systemic lupus erythematosus. *Nat. Med.* 28:2124–2132. https://doi.org/10.1038/s41591-022-02017-5

Mouat, I.C., E. Goldberg, and M.S. Horwitz. 2022. Age-associated B cells in autoimmune diseases. *Cell. Mol. Life Sci.* 79:402. https://doi.org/10.1007/s00018-022-04433-9

Nickerson, K.M., S.R. Christensen, J. Shupe, M. Kashgarian, D. Kim, K. Elkon, and M.J. Shlomchik. 2010. TLR9 regulates TLR7- and MyD88-dependent autoantibody production and disease in a murine model of lupus. *J. Immunol.* 184:1840–1848. https://doi.org/10.4049/jimmunol.0902592

Nickerson, K.M., S. Smita, K.B. Hoehn, A.D. Marinov, K.B. Thomas, J.T. Kos, Y. Yang, S.I. Bastacky, C.T. Watson, S.H. Kleinstein, and M.J. Shlomchik. 2023. Age-associated B cells are heterogeneous and dynamic drivers of autoimmunity in mice. *J. Exp. Med.* 220:e20221346. https://doi.org/10.1084/jem.20221346

Peng, S.L., J. Cappadona, J.M. McNiff, M.P. Madaio, M.J. Owen, A.C. Hayday, and J. Craft. 1998. Pathogenesis of autoimmunity in alphabeta T cell-deficient lupus-prone mice. *Clin. Exp. Immunol.* 111:107–116. https://doi.org/10.1046/j.1365-2249.1998.00424.x

Ricker, E., M. Manni, D. Flores-Castro, D. Jenkins, S. Gupta, J. Rivera-Correa, W. Meng, A.M. Rosenfeld, T. Pannellini, M. Bachu, et al. 2021. Altered

function and differentiation of age-associated B cells contribute to the female bias in lupus mice. *Nat. Commun.* 12:4813. https://doi.org/10.1038/s41467-021-25102-8

Rovin, B.H., R. Furie, K. Latinis, R.J. Looney, F.C. Fervenza, J. Sanchez-Guerrero, R. Maciuca, D. Zhang, J.P. Garg, P. Brunetta, et al. 2012. Efficacy and safety of rituximab in patients with active proliferative lupus nephritis: The lupus nephritis assessment with rituximab study. *Arthritis Rheum.* 64:1215–1226. https://doi.org/10.1002/art.34359

Rovin, B.H., R. Furie, Y.K.O. Teng, G. Contreras, A. Malvar, X. Yu, B. Ji, Y. Green, T. Gonzalez-Rivera, D. Bass, et al. 2022. A secondary analysis of the belimumab international study in lupus nephritis trial examined effects of belimumab on kidney outcomes and preservation of kidney function in patients with lupus nephritis. *Kidney Int.* 101:403–413. https://doi.org/10.1016/j.kint.2021.08.027

Rubtsov, A.V., K. Rubtsova, A. Fischer, R.T. Meehan, J.Z. Gillis, J.W. Kappler, and P. Marrack. 2011. Toll-like receptor 7 (TLR7)-driven accumulation of a novel CD11c^{+} B-cell population is important for the development of autoimmunity. *Blood.* 118:1305–1315. https://doi.org/10.1182/blood-2011-01-331462

Rubtsova, K., A.V. Rubtsov, J.M. Thurman, J.M. Mennona, J.W. Kappler, and P. Marrack. 2017. B cells expressing the transcription factor T-bet drive lupus-like autoimmunity. *J. Clin. Invest.* 127:1392–1404. https://doi.org/10.1172/JCI91250

Sadanaga, A., H. Nakashima, M. Akahoshi, K. Masutani, K. Miyake, T. Igawa, N. Sugiyama, H. Niiro, and M. Harada. 2007. Protection against autoimmune nephritis in MyD88-deficient MRL/lpr mice. *Arthritis Rheum.* 56:1618–1628. https://doi.org/10.1002/art.22571

Sakić, B., H. Szechtman, M. Keffer, H. Talangbayan, R. Stead, and J.A. Denburg. 1992. A behavioral profile of autoimmune lupus-prone MRL mice. *Brain Behav. Immun.* 6:265–285. https://doi.org/10.1016/0889-1591(92)90048-S

Shlomchik, M.J., M.P. Madaio, D. Ni, M. Trounstein, and D. Huszar. 1994. The role of B cells in lpr/lpr-induced autoimmunity. *J. Exp. Med.* 180:1295–1306. https://doi.org/10.1084/jem.180.4.1295

Song, K., L. Liu, X. Zhang, and X. Chen. 2020. An update on genetic susceptibility in lupus nephritis. *Clin. Immunol.* 215:108389. https://doi.org/10.1016/j.clim.2020.108389

Souyris, M., C. Cenac, P. Azar, D. Daviaud, A. Canivet, S. Grunenwald, C. Pienkowski, J. Chaumeil, J.E. Mejia, and J.C. Guery. 2018. TLR7 escapes X chromosome inactivation in immune cells. *Sci. Immunol.* 3:eaap8855. https://doi.org/10.1126/sciimmunol.aap8855

Sthoeger, Z.M., H. Zinger, and E. Mozes. 2003. Beneficial effects of the anti-oestrogen tamoxifen on systemic lupus erythematosus of (NZBxNZW)F1 female mice are associated with specific reduction of IgG3 autoantibodies. *Ann. Rheum. Dis.* 62:341–346. https://doi.org/10.1136/ard.62.4.341

Teichmann, L.L., D. Schenten, R. Medzhitov, M. Kashgarian, and M.J. Shlomchik. 2013. Signals via the adaptor MyD88 in B cells and DCs make distinct and synergistic contributions to immune activation and tissue damage in lupus. *Immunity.* 38:528–540. https://doi.org/10.1016/j.immuni.2012.11.017

Tilstra, J.S., L. Avery, A.V. Menk, R.A. Gordon, S. Smita, L.P. Kane, M. Chikina, G.M. Delgoffe, and M.J. Shlomchik. 2018. Kidney-infiltrating T cells in murine lupus nephritis are metabolically and functionally exhausted. *J. Clin. Invest.* 128:4884–4897. https://doi.org/10.1172/JCI120859

Tilstra, J.S., S. John, R.A. Gordon, C. Leibler, M. Kashgarian, S. Bastacky, K.M. Nickerson, and M.J. Shlomchik. 2020. B cell-intrinsic TLR9 expression is protective in murine lupus. *J. Clin. Invest.* 130:3172–3187. https://doi.org/10.1172/JCI132328

Umiker, B.R., S. Andersson, L. Fernandez, P. Korgaokar, A. Larbi, M. Pilichowska, C.C. Weinkauf, H.H. Wortis, J.F. Kearney, and T. Imanishi-Kari. 2014. Dosage of X-linked Toll-like receptor 8 determines gender differences in the development of systemic lupus erythematosus. *Eur. J. Immunol.* 44:1503–1516. https://doi.org/10.1002/eji.201344283

von Bernuth, H., C. Picard, Z. Jin, R. Pankla, H. Xiao, C.L. Ku, M. Chrabieh, I.B. Mustapha, P. Ghandil, Y. Camcioglu, et al. 2008. Pyogenic bacterial infections in humans with MyD88 deficiency. *Science.* 321:691–696. https://doi.org/10.1126/science.1158298

Wang, C.M., S.W. Chang, Y.J. Wu, J.C. Lin, H.H. Ho, T.C. Chou, B. Yang, J. Wu, and J.Y. Chen. 2014. Genetic variations in Toll-like receptors (TLRs 3/7/8) are associated with systemic lupus erythematosus in a Taiwanese population. *Sci. Rep.* 4:3792. https://doi.org/10.1038/srep03792

Wen, J., J. Doerner, S. Chalmers, A. Stock, H. Wang, M. Gullinello, M.J. Shlomchik, and C. Putterman. 2016. B cell and/or autoantibody deficiency do not prevent neuropsychiatric disease in murine systemic lupus erythematosus. *J. Neuroinflammation.* 13:73. https://doi.org/10.1186/s12974-016-0537-3

Wofsy, D. 1986. Administration of monoclonal anti-T cell antibodies retards murine lupus in BXSB mice. *J. Immunol.* 136:4554–4560. https://doi.org/10.4049/jimmunol.136.12.4554

Wu, W.M., J.L. Suen, B.F. Lin, and B.L. Chiang. 2000. Tamoxifen alleviates disease severity and decreases double negative T cells in autoimmune MRL-lpr/lpr mice. *Immunology.* 100:110–118. https://doi.org/10.1046/j.1365-2567.2000.00998.x

Zhang, Y., J. Liu, C. Wang, J. Liu, and W. Lu. 2021. Toll-like receptors gene polymorphisms in autoimmune disease. *Front. Immunol.* 12:672346. https://doi.org/10.3389/fimmu.2021.672346

Supplemental material

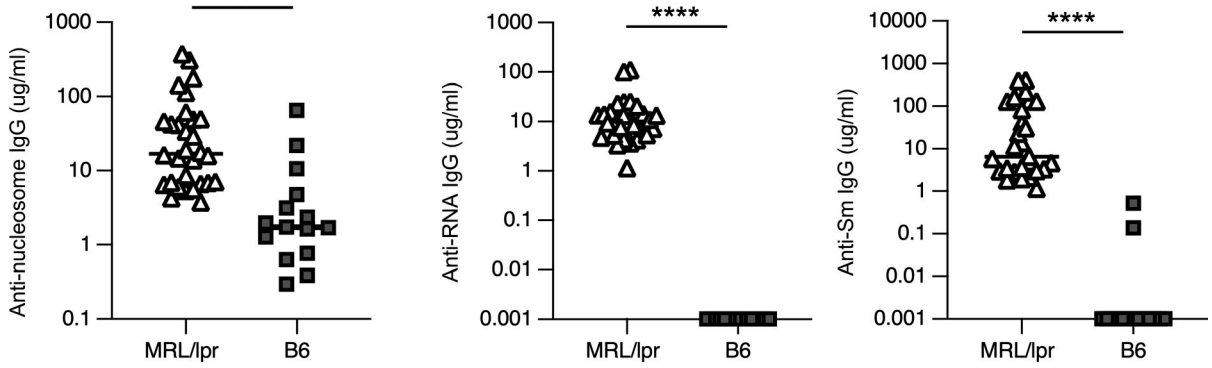

Figure S1. **Autoantibodies are present in 12-wk-MRL.Fas^{lpr} compared with non-autoimmune mice.** Serum concentrations of anti-nucleosome, anti-RNA, and anti-Sm in MRL.Fas^{lpr} (MRL/lpr; *n* = 29–30) and B6 mice (*n* = 15) measured by ELISA at 12-wk of age prior to experimental intervention, Scatter plots display data from individual mice with black lines showing median values, ****P < 0.0001, two-tailed Mann–Whitney *U* test. Data shown are representative of one to two independent cohorts with data combined from all cohorts. *n* is indicated for each experiment as shown.

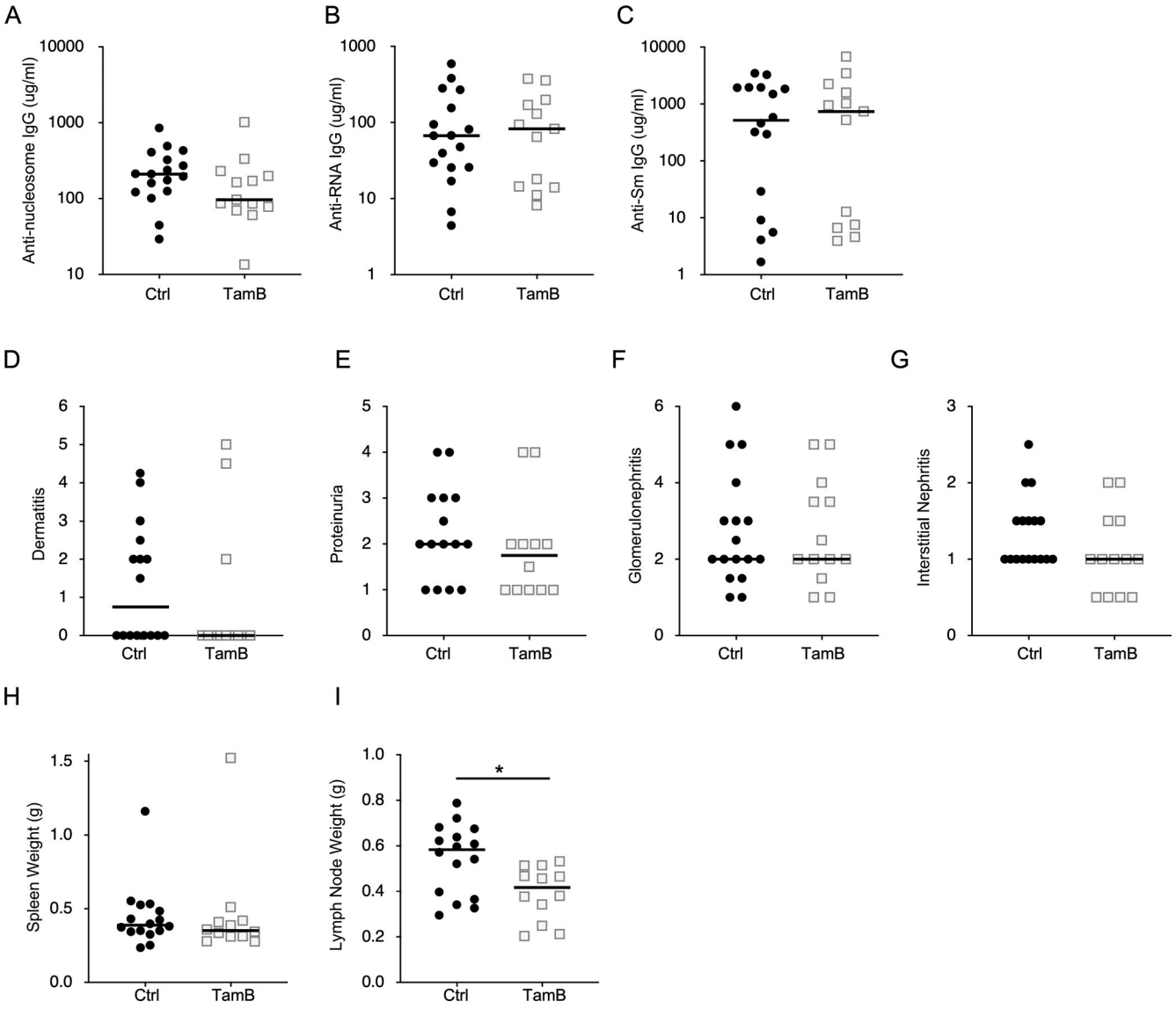

Figure S2. **Activation of Tam-hCD20-Cre alone produced no significant impact on disease phenotype in murine SLE. (A–G)** Serum concentrations of (A) anti-nucleosome, (B) anti-RNA, and (C) anti-Sm were assessed in 20-wk-old male MRL.Fas^{lpr} Cre negative (Ctrl) (n = 17) and Tam-hCD20-Cre (TamB) (n = 13) by ELISA after 8 wk of treatment. Similarly, phenotypic markers of the disease were assessed in this same cohort and included (D) dermatitis, (E) proteinuria, (F) glomerular renal disease, and (G) interstitial and perivascular renal infiltrates. **(H and I)** Additional phenotypic endpoints were assessed for each noted genotype including (H) spleen weight and (I) lymph node weight. Scatter plots display data from individual mice with horizontal lines showing median values. *P < 0.05, two-tailed Mann–Whitney U test. Data shown are representative of two independent cohorts with data combined from all cohorts and n indicated for each experiment as shown.

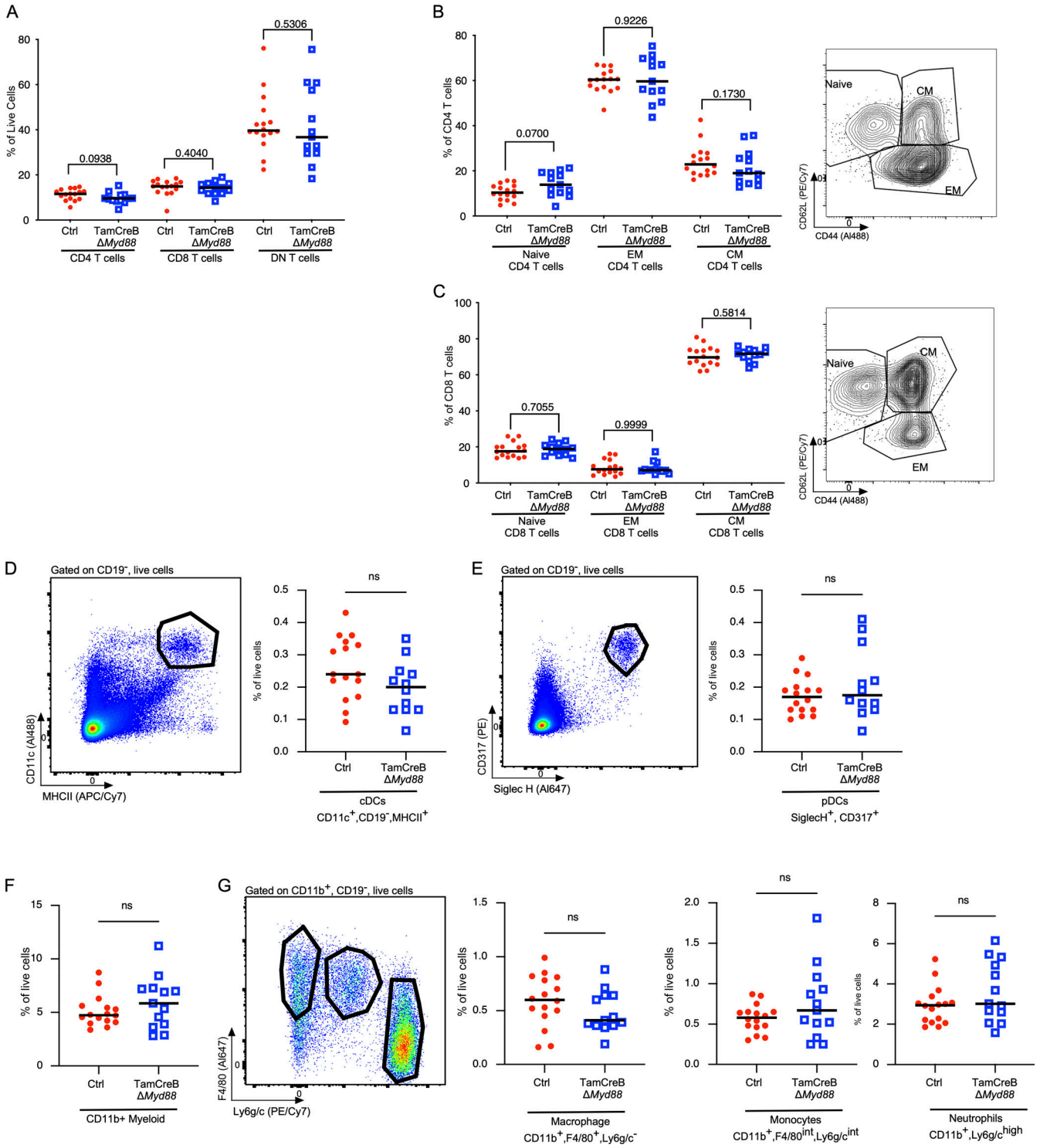

Figure S3. **Myeloid and T cell distribution and activation profile are not significantly different in mice with B cell–specific *Myd88* deletion after disease onset.** The T cell compartment was analyzed for 20-wk-old male Tam-hCD20-Cre;-*Myd88*^{fl} MRL.Fas^{lpr} (TamCreB Δ*Myd88*) (n = 12–13) or Cre negative (Ctrl) (n = 16) MRL.Fas^{lpr} mice after 8 wk of tamoxifen treatment. **(A–C)** Distribution of TCRβ gated population, expressing CD4, CD8, or neither (DN T cells) as a percent of live cells (B) CD4 T cell distributions: naïve (CD62L$^+$, CD44$^-$), central memory T cells (T_{CM}) (CD62L$^+$, CD44$^+$), effector memory T cells (T_{EM}) (CD62L$^-$, CD44$^+$) as a % of TCRβ+CD4$^+$ T cells, with representative FACS plot in the right panel and (C) CD8 T cells distributions: naïve (CD62L$^+$, CD44$^-$), T_{CM} (CD62L$^+$, CD44$^+$), T_{EM} (CD62L$^-$, CD44$^+$) as a % of TCRβ+CD8$^+$ T cells with representative FACS plot in the right panel. **(D)** Distribution of CD11c$^+$, MHCII$^+$, CD19$^-$ cDCs as a percent of live cells with representative FACS plot in the left panel. **(E)** Distribution of CD317$^+$, SiglecH$^+$, CD19$^-$ pDCs as a percent of live cells with representative FACS plot in the left panel. **(F)** Distribution of CD11b$^+$CD19$^-$ myeloid cells. **(G)** Distribution of macrophages CD11b$^+$, F4/80$^+$, Ly6g/c$^-$ macrophages, CD11b$^+$, F4/80^{int}, Ly6g/c^{int} monocytes, and CD11b$^+$, F4/80$^-$, Ly6g/c$^+$ neutrophils as a percent of live cells with representative FACS plot in the left panel. Scatter plots display data from individual mice with horizontal lines showing median values. P values as indicated, using two-tailed Mann–Whitney U test. Data shown are representative of two independent cohorts with data combined from all cohorts and n indicated for each experiment as shown.